Materials Science Forum
ISSN: 1662-9752, Vol. 1185, pp 171-183
doi:10.4028/p-VBNO2g

Submitted: 2026-02-05
Revised: 2026-03-06
Accepted: 2026-03-06
Online: 2026-04-15

Study on the Influence of Gas Pressure Loading Curve on Interface Weld Ratio in Superplastic Forming/Diffusion Bonding of Four-Layer Sandwich Structures

Shengjing Liu[1,a*], Yanhong Mu[1,b], Xiaohua Li[1,c], Hailong Lei[1,d]

[1]AVIC Manufacturing Technology Institute, Beijing 100024, China

[a]sjliu_mti@163.com, [b]muyanhong666@qq.com, [c]13811485985@163.com, [d]lhl_fantasy@126.com

Keywords: Gas pressure loading curve, Superplastic forming/Diffusion bonding (SPF/DB), Interface weld ratio, Void, Four-layer sandwich structure.

Abstract. This paper proposes, for the first time, that the gas pressure loading path significantly influences the weld interface ratio of SPF/DB four-layer sandwich structures. Based on a gas pressure loading curve incorporating back pressure, experimental verification and analysis were conducted. Ultrasonic C-scanning, metallographic examination, and scanning electron microscopy (SEM) were employed to observe and analyze unwelded defects, elucidating their causes and formation mechanisms. Key process parameters—including back pressure time, back pressure value, and gas inlet delay time—were extracted and defined. The influence of these parameters on the weld interface ratio of four-layer sandwich structures was systematically investigated. Finally, with the objectives of eliminating surface grooves and achieving a high weld interface ratio, reference ranges for these process parameters are provided.

Introduction

With the advancement of aerospace technology, structural components are increasingly required to exhibit high integrity, specific strength, forming accuracy, temperature resistance, and cost-effectiveness. Titanium alloy superplastic forming/diffusion bonding (SPF/DB) technology offers a viable solution to meet these demands.

At elevated temperatures around 900°C, titanium alloys exhibit low deformation resistance and excellent ductility, enabling simultaneous precision forming against a die and solid-state diffusion bonding under argon gas pressure. The SPF/DB process is characterized by its simplicity, flexibility in stiffener layout design, and capability to integrally form complex, lightweight, and high-strength components with tight dimensional tolerances—making it a representative near-net-shape manufacturing technique.

The SPF/DB process enables the production of hollow multilayer titanium alloy structures that are difficult or impossible to fabricate using conventional methods. To date, various configurations have been successfully developed worldwide, including single-layer components such as frames and caps; double-layer structures such as doors, panels, and covers; three-layer components such as wide-chord fan blades; and four-layer structures including fins, fairings, main landing gear doors, wing access panels, and airfoil components.

In recent years, four-layer sandwich structures manufactured by SPF/DB have found increasing application in aerospace vehicles due to their efficient material utilization and superior load-bearing capacity. However, due to limitations inherent in the forming process and structural design, achieving a high weld interface ratio remains a critical technical challenge that restricts the qualification rate and broader application of these structures. This issue directly affects the load-bearing strength, fracture toughness, and fatigue performance of the final product.

The weld interface ratio in titanium alloy SPF/DB four-layer sandwich structures is influenced by several key factors, including diffusion bonding temperature, pressure, holding time, surface condition, environmental atmosphere, and material microstructure. Numerous studies have systematically investigated these parameters, identifying their individual effects on the weld interface ratio and establishing optimal process windows through experimental validation.

Nevertheless, the influence of the gas pressure loading curve on the weld interface ratio of SPF/DB four-layer structures has not been previously explored. This paper presents, for the first time, the significant role of the gas pressure loading curve in determining the weld interface ratio. Through experimental process optimization, four-layer test specimens with a weld interface ratio of 95% or higher were successfully obtained.

Experimental Materials and Methods

Experimental Materials

The experiment utilized TC4 titanium alloy, a medium-strength α+β duplex-phase fine-grained alloy. Due to its high strength, excellent corrosion resistance, good weldability, and biocompatibility, TC4 is widely used in aerospace, medical, and chemical fields. TC4 exhibits good superplasticity and diffusion bonding performance at elevated temperatures ranging from 890°C to 930°C.

Microstructural analysis of the as-received material with a thickness of 0.6mm was conducted. Average values from four test groups are presented in Table 1. The sheet surfaces were bright, flat, and free from scratches or visible pitting.

Table1. Microstructure and Properties of Ti-6Al-4V Sheet

Microstructure State	Microstructure State Grain Size	Composition (%)						
		Al	V	Fe	C	N	H	O
Equiaxed duplex	Grade 14	5.76	4.02	0.16	0.019	0.008	0.0035	0.128

Experimental Methods

The primary process parameters affecting SPF/DB quality are temperature, pressure, and time. The SPF equipment used in this study features precise temperature control, automatic gas pressure loading control, and mechanical pressure loading systems, along with corresponding automatic detection, recording, and signal feedback systems. This enables accurate control of temperature, gas pressure loading curve, and mechanical pressure.

A typical SPF/DB process for a four-layer sandwich structure is illustrated in Fig. 1. When the mold temperature reaches SPF conditions, argon gas is introduced into the outer layer, forming the outer skin against the die. After a holding period, diffusion bonding is completed at the areas of the inner skin not coated with stop-off agent. The outer layer pressure is then released, and gas is introduced into the inner layer. The inner skin undergoes superplastic forming to create the stiffener structure. Finally, after another holding period, the triangular regions of the stiffeners progressively reduce, and the contact area between the inner and outer skins gradually increases, ultimately completing diffusion bonding both between the inner and outer skins and within the stiffener regions.

From the above analysis, it is evident that the diffusion bonding process between the inner and outer skins is complex. When gas is introduced into the outer layer, a vacuum condition cannot be maintained; otherwise, "full-groove" surface forming defects would appear. The diffusion bonding process occurs concurrently with the stiffener forming process. Shear stress exists between the sheets, characteristic of dynamic diffusion bonding, which tends to result in a relatively poor weld interface ratio and makes the process prone to poor bonding and surface groove defects. In summary, the pressure path effects are particularly critical in four - layer structures.

To improve forming efficiency and the quality stability of stiffener diffusion bonding, a process sequence involving initial core sheet diffusion bonding followed by SPF/DB of the four-layer structure was adopted. The specific process flow is: sheet blanking → degreasing and pickling → pattern preparation → core sheet pocket sealing welding → core sheet diffusion bonding → core sheet cutting → alkali etching and pickling → four-layer pocket sealing welding → four-layer structure SPF/DB. Methods such as degreasing and pickling or alkali etching and pickling are

employed during the process to remove surface oil stains and other impurities, ensuring the cleanliness required for the surfaces to be diffusion bonded.

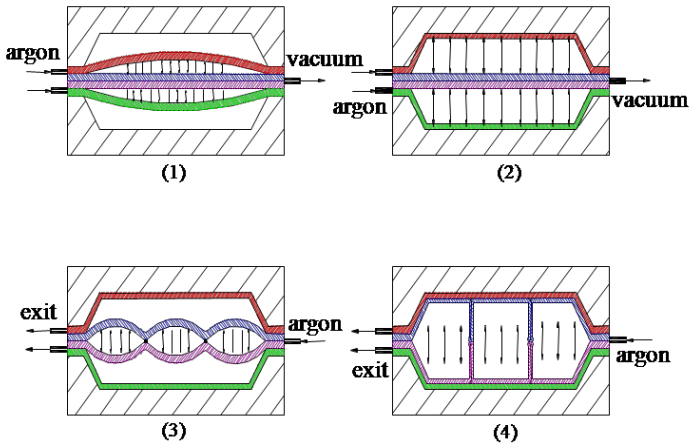

Fig.1 SPF/DB process for four-layer sandwich structure

The four-layer SPF/DB test specimen measures 400 mm in length and 300 mm in width. After superplastic forming, the cavity height between the inner sheets is 8-10 mm.The argon gas purity used for the repeated tests was 99.99%.

Experimental research indicates that during SPF/DB, a gas pressure loading curve based on back pressure can reduce premature local adhesion between the inner and outer skins and effectively suppress surface groove defects in four-layer structures. As shown in Fig. 2, the gas pressure loading curve developed by the SPF/DB team at AVIC Manufacturing Technology Institute, based on years of process development and accumulated experience, effectively suppresses the occurrence of surface grooves.

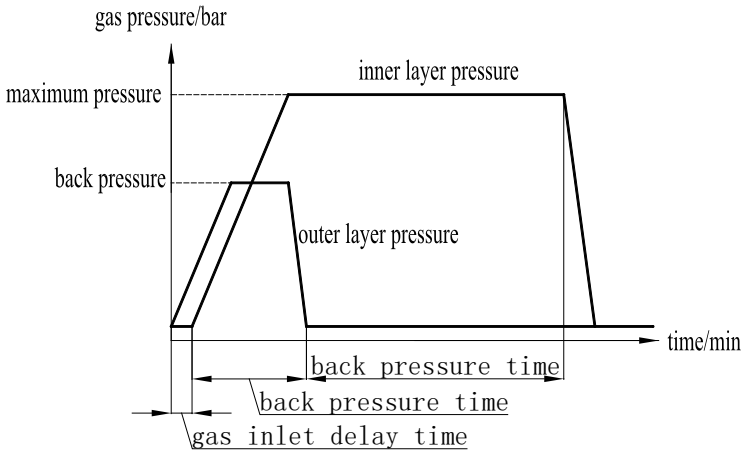

Fig.2 Gas pressure loading curve based on back pressure

To ensure part forming quality and facilitate research, other process parameters were fixed as follows: SPF/DB temperature at 910°C ± 5°C, maximum inner layer pressure at 21 bar, holding time at 140 min, inner/outer layer pressurization rate at 0.78 bar/min, and inner/outer layer depressurization rate at 2.3 bar/min.After the back pressure was released, during the holding stage, the outer sheet gas pressure was maintained at 1.0-1.2 bar to prevent surface groove defects.

After SPF/DB completion, ultrasonic C-scanning and metallographic examination were used to analyze the diffusion bonding quality at the four-layer structure interface. Scanning electron microscopy (SEM) was employed for morphological observation and compositional analysis at diffusion bonding defect locations.

Analysis of Experimental Results

Analysis of Unwelded Defects

Currently, the effective technical method for detecting unwelded defects is ultrasonic testing, which automatically calculates the weld ratio based on the ratio of the cumulative area of defects shown in the image to the total area of the part.The core of converting ultrasonic C-scan data into welded/unwelded areas lies in threshold calibration. This process essentially involves binarizing the collected continuous ultrasonic signals (such as amplitude and wave height) by setting one or more critical values, thereby distinguishing between "acceptable" and "defective" areas.

In this experimental procedure, the C-scan was performed using a 50 MHz probe frequency with a 0.5 mm step size. Calibration was performed using a reference specimen with a φ0.8 mm flat-bottomed hole, made of the same material as the workpiece to be inspected. After the specimen was certified as qualified by a third-party inspection agency, it was used as the basis for calibration. The probe was focused on the defect location in the standard reference block, and the scanning depth and amplitude were adjusted. The amplitude of the reflected wave generated by the defect was adjusted to approximately 95% of the full screen height, and the defect wave identification threshold was set at 90%. This established the correspondence between defect size and the C-scan image.

With an gas inlet delay time of 5 min, a back pressure value of 13 bar, and a back pressure time of 50 min, typical ultrasonic detection results for interface unwelded defects are shown in Fig. 3. The unwelded defects appear nearly circular and are uniformly and dispersedly distributed along the diffusion interface. However, within 10 mm on either side of the stiffeners, the weld interface ratio is good.

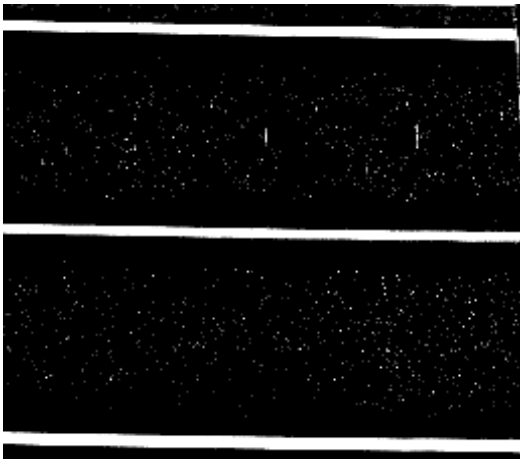

Fig.3 Ultrasonic detection results of interface unwelded defects

Samples from the unwelded area were extracted using high-pressure water jet cutting for supplementary metallographic examination. The metallographic analysis morphology is shown in Fig. 4. The microstructure consists of equiaxed primary α + β, with an α phase content of no less than 50%. No oxide layer or α-rich layer was observed at the diffusion bonding interface or within unwelded areas. The metallographic analysis results show good consistency with the ultrasonic non-destructive testing results. The unwelded defects are approximately circular, with sizes ranging from Φ1 μm to Φ5 μm.

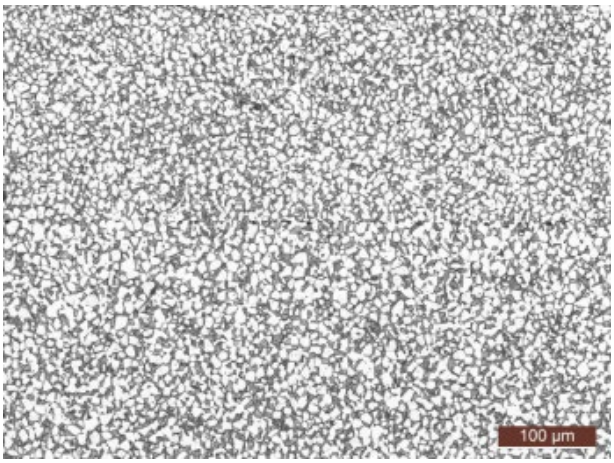

Fig.4 Metallographic examination results of interface unwelded defects

To further determine the cause of the unwelded defects, additional verification tests were conducted. The diffusion bonding quality at the leading-edge position of the test specimen exhibiting interface unwelded defects was analyzed and tested. The weld interface ratio consistently exceeded 95%, ruling out the influence of material microstructure, temperature, time, and blank surface condition on the dispersive interface unwelded defects. During SPF/DB, the space between the inner and outer skins was maintained under vacuum while keeping other parameters unchanged. The interface diffusion bonding quality of the resulting specimens was analyzed and tested, and their weld interface ratios all exceeded 95%, ruling out the influence of diffusion pressure on the unwelded defects. It is concluded that the defects are closely related to the argon gas present between the inner and outer layers.

To confirm whether the argon gas was contaminated by oxygen or other impurities, SEM observation was performed on typical unwelded defects. A representative morphology of an unwelded defect is shown in Fig. 5. Spectrum analysis was conducted at four locations within the SEM observation area. Locations 1, 2, and 4 correspond to unwelded defect composition analysis, while location 3 represents the average composition analysis of the base microstructure. The spectrum analysis results are shown in Fig. 6, with statistical analysis provided in Table 2. The SEM spectrum analysis results indicate that the main elemental compositions at all four locations are Ti, Al, and V, with no oxygen or other impurity elements detected. The Al content at locations 1 and 2 is higher than at location 4, while the V content is lower. It is inferred that locations 1 and 2 correspond to the α phase, and location 4 corresponds to the β phase. Location 3 represents the average of the base microstructure, with elemental content falling in the intermediate range.

The SEM analysis concludes that the unwelded area exhibits typical void morphology, free from oxides or other impurities.

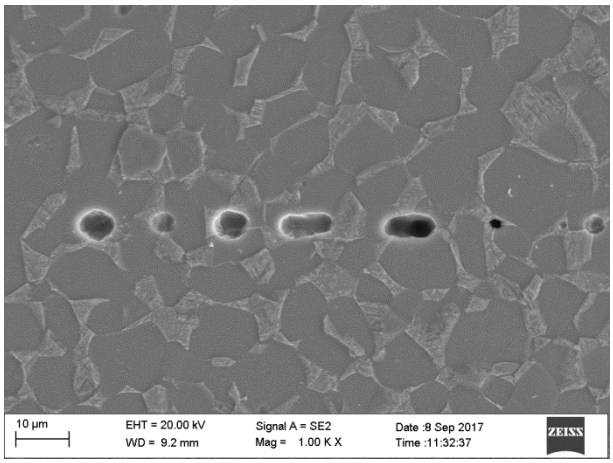

(a) Low-magnification image

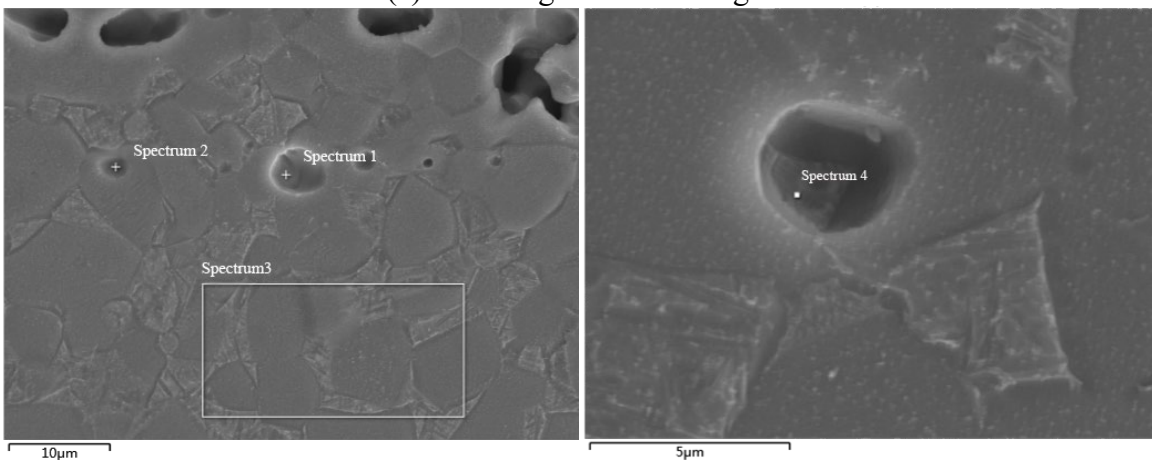

(b) Marking of spectrum analysis locations

Fig. 5 SEM images of interface unwelded defects

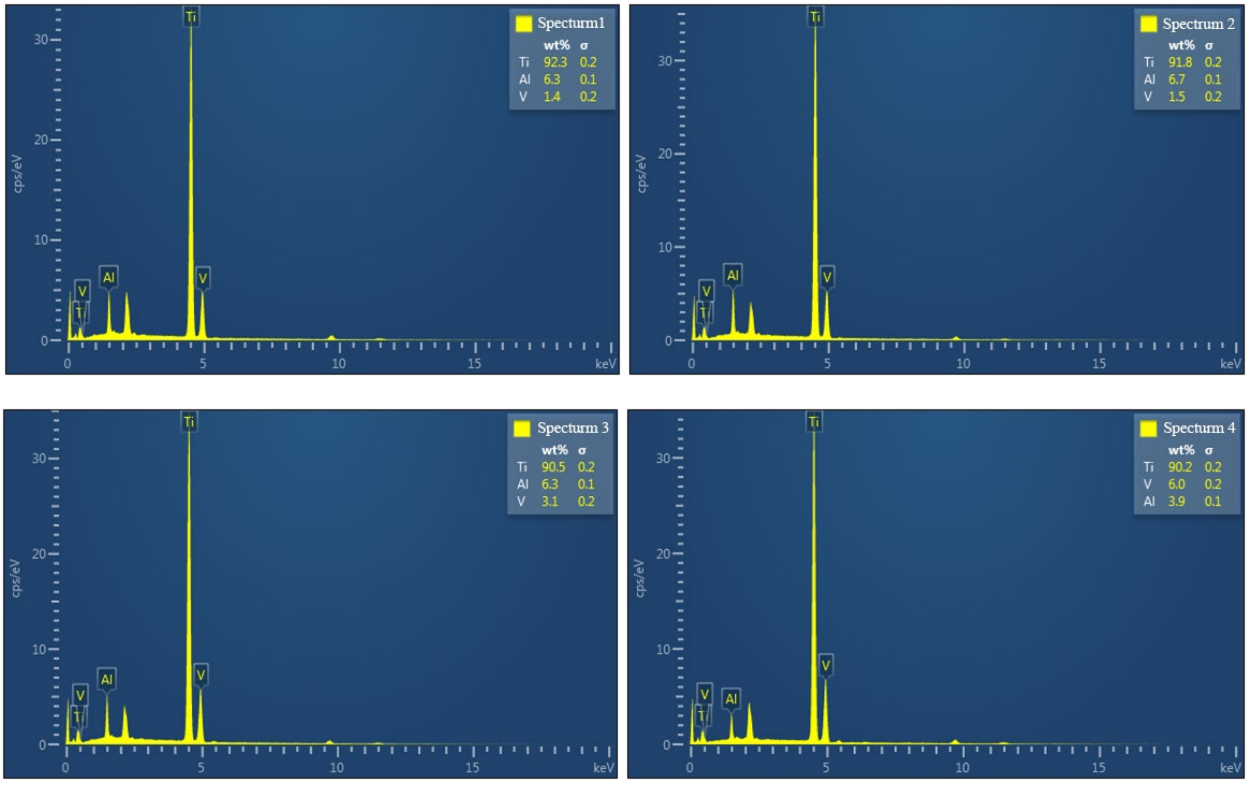

Fig.6 SEM spectrum analysis results

Table 2 Composition percentages from SEM spectrum analysis

Spectrum Label	Spectrum 1	Spectrum 2	Spectrum 3	Spectrum 4
Al	6.32	6.67	6.34	3.86
Ti	92.30	91.81	90.54	90.19
V	1.38	1.52	3.12	5.96
Total	100	100	100	100

Voids are inevitable intermediate products during the diffusion bonding process and have been extensively studied. The diffusion bonding process generally consists of three stages: (1) Local areas of the interface enter the physical contact stage under plastic and viscoplastic deformation mechanisms; (2) Under diffusion pressure and temperature, atoms become activated, and initial contact areas at the interface begin to form chemical bonds, such as metallic bonds, leading to the appearance of voids; (3) Under surface source and interface source mechanisms, atoms undergo interface and volume diffusion, causing voids to continuously shrink and gradually disappear, ultimately forming a reliable diffusion-bonded interface.

It is inferred that during SPF/DB of the four-layer structure, under the influence of outer layer pressure and the pressure differential between inner and outer layers, the inner and outer skins gradually form against the die and come into local contact. In the second stage of diffusion bonding, approximately dispersed closed voids form at the diffusion interface. Before this stage commences, if the gas from the outer layer cannot be promptly vented, it becomes sealed within these voids. During the third stage, under surface source and interface source mechanisms, atomic interface and volume diffusion occur, causing the voids to shrink continuously. The internal residual gas pressure gradually increases, eventually reaching equilibrium with the force from diffusion mechanisms. At this point, void shrinkage stagnates, resulting in unwelded defects.

The triangular stiffener areas are the last to form. When closed voids form at these locations, the back pressure has already been vented, leaving no residual gas inside the voids. Consequently, within 10 mm on either side of the triangular stiffener area, the interface weld ratio is good.

Influence of Back Pressure Time on Interface Weld Ratio

With an gas inlet delay time of 5 min and a back pressure value of 13 bar, back pressure time was set to 20 min, 30 min, 40 min, 50 min, and 60 min, respectively. The ultrasonic detection results for interface weld ratio corresponding to different back pressure time is shown in Fig. 7. The influence of back pressure time on interface weld ratio, derived from these results, is presented in Fig. 8.

Experimental results show that when back pressure time $\leq$ 30 min, the interface weld ratio is $\geq$ 95%. When back pressure time > 30 min, the interface weld ratio gradually decreases with increasing back pressure time, initially with a gentle decline. Between 50 and 60 min, the interface weld ratio drops rapidly from 80% to approximately 50%. Unwelded defects appear as dispersed spots, relatively uniformly distributed along the diffusion bonding interface. Within 10 mm on both sides of the stiffeners, the weld ratio remains good.

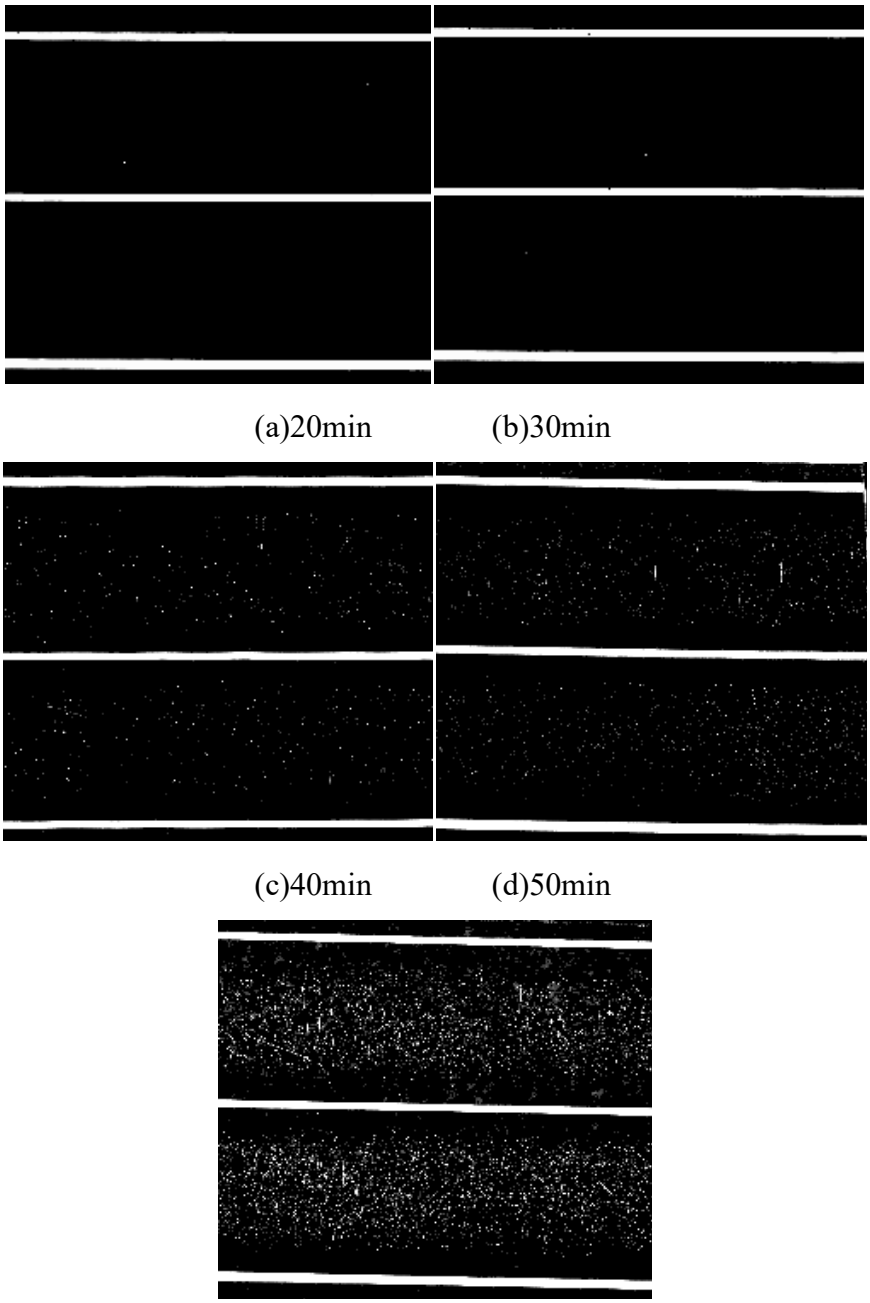

(a)20min (b)30min

(c)40min (d)50min

(e)60min

Fig.7 Ultrasonic detection results of diffusion bonding quality under different back pressure time conditions

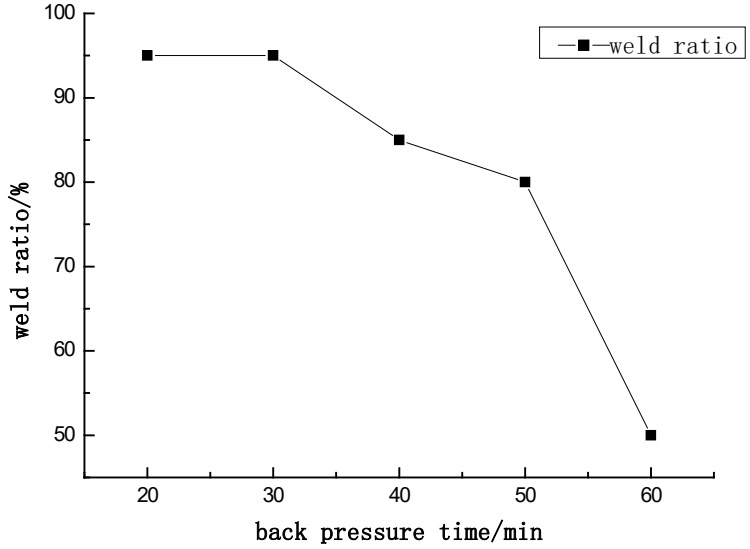

Fig.8 Analysis of the influence of back pressure time on interface weld ratio

The metallographic analysis morphologies corresponding to different back pressure time is shown in Fig. 9. No oxide layer or α-rich layer was observed at the diffusion bonding interface or within unwelded areas. The metallographic analysis results show good consistency with the ultrasonic non-destructive testing results. When the back pressure time exceeds 30 minutes, metallographic analysis results show that void-type lack of fusion defects begin to appear at the interface to be diffused, and the length of the void line increases with longer back pressure time. When the weld ratio is high, unwelded defects are nearly circular, with sizes ranging from Φ1 μm to Φ8 μm. When the weld ratio is low, unwelded defects are elliptical or elongated, with the long axis oriented along the diffusion interface, reaching a maximum length of approximately 10 μm.

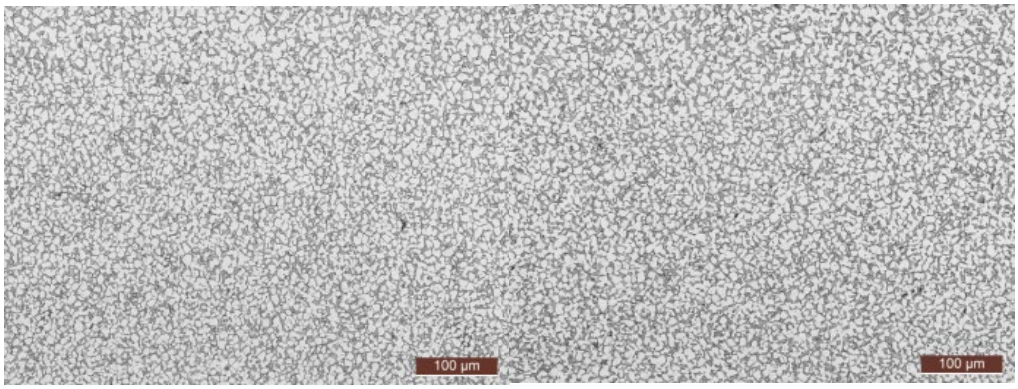

(a)20min (b)30min

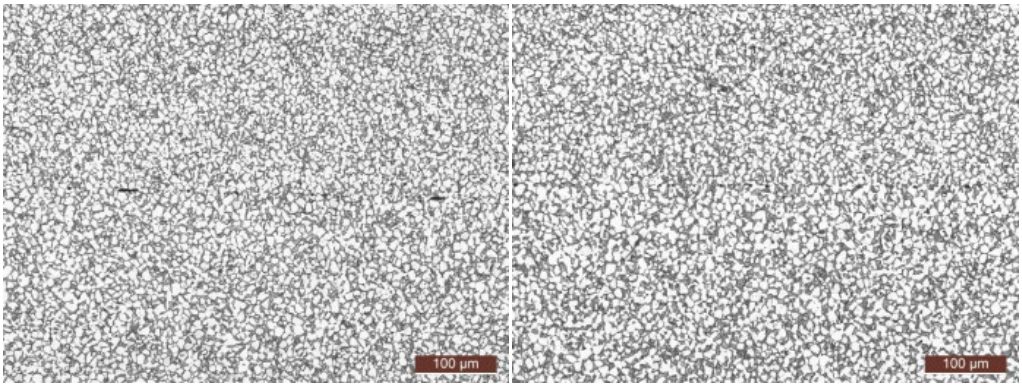

(c)40min (d)50min

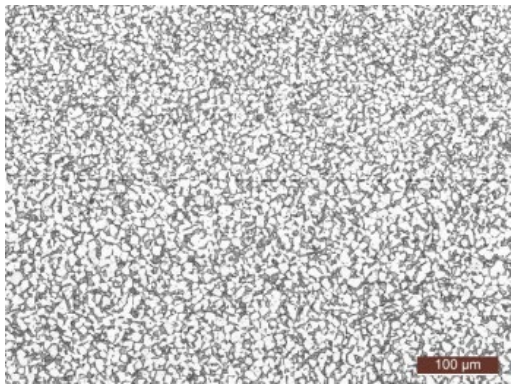

(e)60min

Fig.9 Metallographic examination results of diffusion bonding quality under different back pressure time conditions

It is inferred that as back pressure time increases, the difficulty of venting gas from the outer layer gradually increases, leading to a continuous increase in the amount of residual gas trapped within the voids. Consequently, the void volume at shrinkage stagnation becomes larger, and voids do not have sufficient time to evolve into multiple smaller voids, typically appearing elliptical or elongated. Ultimately, the area of unwelded interface defects increases, and the weld ratio deteriorates.

Influence of Back Pressure Value on Interface Weld Ratio

With an gas inlet delay time of 5 min, back pressure time was set to 20 min, 30 min, 40 min, 50 min, and 60 min, respectively. For each back pressure time, back pressure values were set to 3 bar, 8 bar, 13 bar, and 18 bar. The influence of different back pressure values on the interface weld ratio was experimentally analyzed for each back pressure time.

Experimental results show that when the back pressure values were 3 bar and 18 bar, respectively, surface grooves of varying sizes appeared at local positions on the parts for different back pressure time. It is inferred that when the back pressure value is low, the lubricating effect is insufficient, leading to premature local adhesion between the inner and outer skins during SPF/DB. As the stiffeners form, the outer skin in the adhered areas is pulled by the inner skin, forming surface grooves. When the back pressure value is high, gas inlet uniformity on the upper and lower sides is compromised, making the inner skin prone to uneven deformation, which can cause unilateral adhesion and result in surface grooves.

The influence of back pressure value on interface weld ratio is shown in Fig. 10. Ultrasonic non-destructive testing and metallographic results indicate that the morphology and distribution of unwelded defects are similar to those previously described. Analysis of experimental results shows that when the back pressure time $\leq$ 30 min, under different back pressure conditions, the interface weld ratio remains good, all $\geq$ 95%. When the back pressure time exceeds 30 min, under the same back pressure time condition, the interface weld ratio increases with increasing back pressure value, with this effect being particularly pronounced at longer back pressure time.

It is inferred that under the same back pressure time condition, an increase in back pressure value reduces the pressure differential between the inner and outer layers, slowing the deformation rate of the inner skin and delaying the contact time between the inner and outer skins (equivalent to a reduction in effective back pressure time). This reduces the amount of gas sealed within the voids, ultimately improving the interface weld ratio.

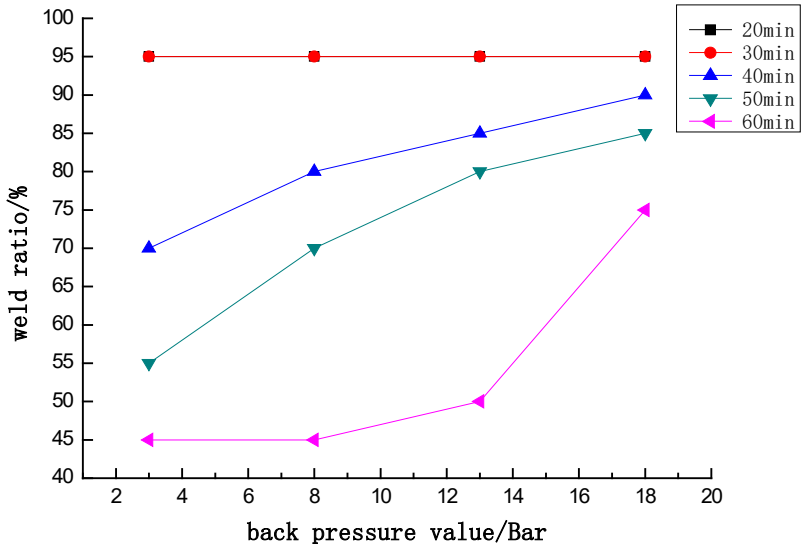

Fig.10 Analysis of the influence of back pressure value on interface weld ratio

Influence of Gas Inlet Delay Time on Interface Weld Ratio

With a back pressure value of 13 bar, back pressure time was set to 20 min, 30 min, 40 min, 50 min, and 60 min, respectively. For each back pressure time, gas inlet delay time was set to 0 min, 5 min, 10 min, and 15 min. The influence of different gas inlet delay time on the interface weld ratio was experimentally analyzed for each back pressure time.

Experimental results show that when the gas inlet delay time was 0 min and 15 min, respectively, surface grooves of varying sizes appeared at local positions on the parts for different back pressure time. It is inferred that when the gas inlet delay time is 0 min (i.e., simultaneous inner and outer layer gas inlet), the gap between the inner and outer skins is small, making local adhesion and subsequent surface groove formation more likely. When the gas inlet delay time is long, the coordinated action of gas inlet into the inner and outer cavities becomes less effective. Under the initial back pressure, the inner skin is prone to uneven deformation, which can cause local adhesion and lead to surface grooves.

The influence of gas inlet delay time on the interface weld ratio is shown in Fig. 11. Ultrasonic non-destructive testing and metallographic results show that the morphology and distribution of unwelded defects are similar to those previously described. Experimental results show that when the back pressure time $\leq$ 30 min, under different gas inlet delay time conditions, the interface weld ratio is $\geq$ 95%. When the back pressure time exceeds 40 min, the interface weld ratio improves with increasing gas inlet delay time.

It is inferred that when the inner skin initially deforms upon gas inlet, the back pressure increases, the deformation rate decreases, and the contact time between the inner and outer skins is relatively delayed (equivalent to a reduction in effective back pressure time). This reduces the amount of gas sealed within the voids, thus improving the interface weld ratio.

Analysis and Discussion of Other Influencing Factors

Factors such as the wall thickness of the inner and outer layers of the four-layer structure, the height of the stiffeners within the cavity, and the design of the inlet/outlet channels are also likely to significantly influence the interface weld ratio and the occurrence of surface grooves, potentially interacting with the parameters investigated in this study.

All results presented in this paper were obtained under fixed conditions for the above-mentioned factors. Due to space limitations, a detailed discussion and analysis of these additional influencing factors are not provided here.

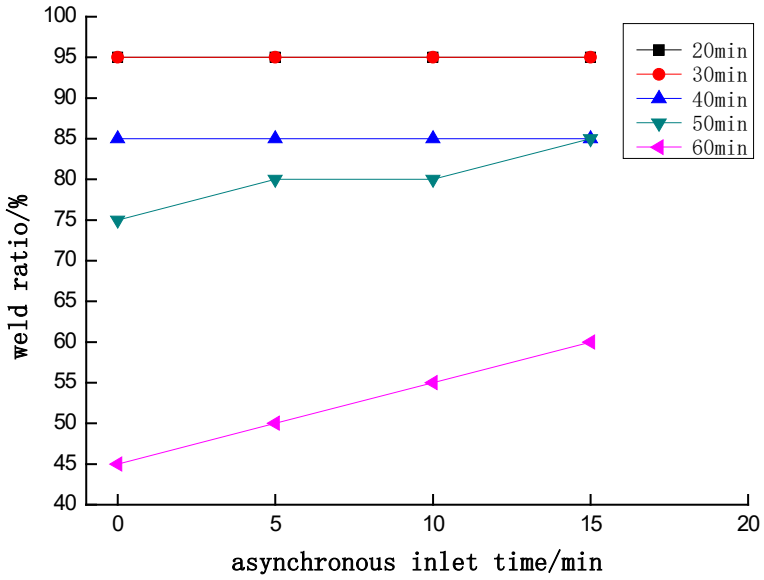

Fig.11 Analysis of the influence of gas inlet delay time on interface weld ratio

Summary

(1) The gas pressure loading curve based on back pressure can effectively suppress surface groove defects in four-layer structures but significantly influences their interface weld ratio. Dispersed spot-like unwelded defects are primarily distributed between the inner and outer skins that come into contact first. The triangular stiffener areas contact and form during the final stage. If the back pressure has been vented to a low level by this time, the interface weld ratio in these areas remains good.

(2) When back pressure time exceeds 40 min, gas from the outer layer cannot be vented in a timely manner and becomes trapped within closed voids. These voids appear approximately circular and are uniformly dispersed at the diffusion interface, ultimately forming unwelded defects.

(3) When back pressure time exceeds 40 min, as back pressure time increases, the amount of residual gas trapped within the voids increases, leading to a decrease in the interface weld ratio.

(4) When back pressure time exceeds 40 min, under the same back pressure time condition, an increase in either the back pressure value or the gas inlet delay time reduces the deformation rate of the inner skin and delays the contact time between the inner and outer skins (equivalent to a reduction in effective back pressure time), thereby improving the interface weld ratio.

(5) When the back pressure value is maintained between 8 and 13 bar, the back pressure time between 20 and 30 min, and the gas inlet delay time between 5 and 10 min, the fabricated four-layer structure components are free of surface grooves and exhibit an interface weld ratio of 95% or higher.

References

[1] Li Zhiqiang, Wang Xiangnian. Development Status and Prospects of Aviation Manufacturing Technology [J]. International Aviation, 2014, 8:52-55.

[2] Liu Shengjing, Xu Yongchao, Jiang Bo, Lei Hailong, Chen Fulong. Mechanical Analysis of Superplastic Free Bulging Based on Ellipsoidal Surface [J]. Journal of Mechanical Engineering, 2014, (18):73-81.

[3] Li Zhiqiang, Guo Heping. Application Progress and Development Trend of Superplastic Forming/Diffusion Bonding Technology [J]. Aeronautical Manufacturing Technology, 2010, 8:32-35.

[4] Liu Shengjing, Lei Hailong, Chen Fulong. Analysis of Bulging Mechanism in Superplastic Forming/Diffusion Bonding Four-Layer Sandwich Structures [J]. Forging & Stamping Technology, 2014, (08):30-36.

[5] Li Zhiqiang. Titanium Alloy Superplastic Forming/Diffusion Bonding Four-Layer Sandwich Structure [J]. Aviation Science and Technology, 1995, 6:23-24.

[6] Gao Wenjing, Lei Junxiang. Application and Research Progress of Diffusion Bonding Technology in Titanium Alloy Processing [J]. Nonferrous Metal Materials and Engineering, 2017, 4:239-246.

[7] FA Calvo, JMGD Salazar, A Urena, et al. Diffusion bonding of Ti-6Al-4V alloy at low temperature: metallurgical aspects [J]. Journal of Materials Science, 1992, 27(2):391-398.

[8] Lee H S, Yoon J H, Yi Y M. Oxidation Behavior of Titanium Alloy under Diffusion Bonding [J]. Thermochimica Acta, 2007, 455(1/2):105-108.

[9] Sanders D G, Ramulu M. Examination of superplastic forming combined with diffusion bonding for titanium: Perspective from experience [J]. Journal of Materials Engineering and Performance, 2003, 13(6):744-752.

[10] Ma Ruifang, Li Miaoquan, Li Hong, Yu Weixin. A Void Closure Model Based on Kinetic Conditions of Metal Diffusion Bonding Mechanism [J]. Scientia Sinica, 2012, 9:1081-1091.

[11] Guo Wei, Zhao Xihua, Song Minxia. Current Status and Development of Diffusion Bonding Interface Theory [J]. Aerospace Manufacturing Technology, 2004, 5:36-39.